Journal of Power Sources 216 (2012) 36–41

Contents lists available at SciVerse ScienceDirect

Journal of Power Sources

journal homepage: www.elsevier.com/locate/jpowsour

Organic and inorganic surface passivations of TiO_2 nanotube arrays for dye-sensitized photoelectrodes

Hun Park [a], Changduk Yang [b], Won-Youl Choi [c,*]

[a] Photovoltaic Research Department, Green Energy Research Institute, Hyundai Heavy Industries Co., Ltd., Yongin 446-912, Republic of Korea
[b] Interdisciplinary School of Green Energy, Ulsan National Institute of Science and Technology, Ulsan 689-798, Republic of Korea
[c] Department of Metal and Materials Engineering, Gangneung-Wonju National University, Gangneung 210-720, Republic of Korea

HIGHLIGHTS

- TiO_2 nanotube arrays as photoelectrode in DSCs.
- Organic passivation layer for TiO_2 nanotube arrays.
- Inorganic passivation layer for TiO_2 nanotube arrays.
- Power conversion efficiency is improved by passivation layer.

ARTICLE INFO

Article history:
Received 26 March 2012
Received in revised form
12 May 2012
Accepted 21 May 2012
Available online 28 May 2012

Keywords:
Dye-sensitized solar cells
Titanium dioxide
Nanotube
Surface passivation

ABSTRACT

Surface passivation of photoelectrodes is widely used to improve the performance of dye-sensitized solar cells (DSCs). We use the organic and inorganic materials as a surface-passivating layer of photoelectrodes and introduce the effect of surface passivation on the power conversion efficiency of DSCs. TiO_2 nanotube arrays are fabricated by anodic oxidation of Ti foil for photoelectrodes of DSCs. Surface passivating layers are conducted by immersing photoelectrode in various precursor solutions. MgO and WO_3 are selected for inorganic passivation. $PC_{61}BM$ is used for organic passivation. In case of inorganic passivation, a basic material (MgO) which has a high isoelectric point (pI >7) shows higher power conversion efficiency of 2.63% by increasing of open circuit voltage (V_{oc}) to 0.74 V than bare sample of 2.55%. But, an acidic material (WO_3) shifts V_{oc} to low potential resulting in a worse efficiency of DSCs. In case of organic passivation, $PC_{61}BM$ enhances photocurrents and decreases V_{oc} value compared to bare sample. The power conversion efficiency of $PC_{61}BM$-coated DSCs is overall improved due to enhanced photocurrents despite of V_{oc} offset to low potential. Back-transfer electron blocking, dye adsorption, TiO_2 conduction band shifting, and additional charge generation by surface passivation are discussed.

1. Introduction

Dye-sensitized solar cells (DSCs) have a great potential as alternative photovoltaic devices for silicon or CIGS solar cells due to their low cost and easy fabrication [1]. However, relatively low efficiency (11.2%) [2] has been a drawback for successful commercialization of DSCs. TiO_2 nanoparticle structure, which shows the best efficiency for DSCs, has a disordered structure at the contact of nanocrystalline particles. This disordered state hinders the charge transport by diffusion in TiO_2 films, thus limiting further improvement of power conversion efficiency of DSCs [3,4].

Several nanostructures such as nanotubes [3,5–10], nanorods [11], nanowires [12], nanohemispheres [13], etc. have been studied to find an alternative for TiO_2 nanoparticle structure. Recently, highly ordered TiO_2 nanotube arrays have received a great attention due to their one dimensional (1-D) structure and low charge recombination [3–10,14]. In TiO_2-nanotube-based DSCs compared to TiO_2-nanoparticle-based DSCs, superior power conversion efficiency and longer electron lifetime have been reported when TiO_2 film thickness was same [6,7]. However, the optimized efficiency for TiO_2-nanotube-based DSCs is still lower than that of TiO_2-nanoparticle-based DSCs. More efforts and trials should be concentrated on the further improvement of power conversion efficiency for TiO_2-nanotube-based DSCs.

Surface passivation of TiO_2 photoelectrodes has been widely used in an application to DSCs not only to minimize charge loss at

* Corresponding author. Tel.: +82 33 640 2483; fax: +82 33 642 2245.
E-mail address: cwy@gwnu.ac.kr (W.-Y. Choi).

0378-7753/$ – see front matter © 2012 Elsevier B.V. All rights reserved.
doi:10.1016/j.jpowsour.2012.05.060

the interface of TiO_2 film and liquid electrolyte, but also to enhance dye adsorption [5,8,9,15–19]. High band gap (E_g) oxides such as MgO [8,19], $SrTiO_3$ [16,18], ZnO [5], WO_3 [15], etc. were selected for surface-passivating materials, because the position of conduction band for surface-passivating materials should be higher than that of TiO_2 conduction band. Higher position of conduction band for surface-passivating materials blocks the back-transfer of injected photoelectrons, hence reducing charge recombination rate. The thickness of surface-passivating layers was controlled to optimized value. When the thickness of surface-passivating layers is too thick, charge injection from dye molecules to TiO_2 film can be hindered and photocurrent is reduced [8]. The concept of isoelectric point [20] was used to select surface-passivating materials and to interpret the effect of interlayer between TiO_2 film and liquid electrolyte [9,17,19]. Basic coating layers, which have high isoelectric points (>7), enhance dye adsorption and shift TiO_2 conduction band in the negative direction. Enhanced dye adsorption increases charge injection of photoelectrons and the shifting of TiO_2 conduction band in the negative direction improves photovoltage, which is the difference of energy level between TiO_2 conduction band and liquid electrolyte. On the other hand, acidic coating layers, which have low isoelectric point (<7), have a minor effect on the dye adsorption or shift TiO_2 conduction band in the positive direction.

In this work, we introduce surface passivation with organic and inorganic materials to improve the power conversion efficiency of TiO_2-nanotube-based DSCs. MgO and WO_3 were selected as inorganic surface-passivating materials, and $PC_{61}BM$ ((6,6)-phenyl C_{60} butyric acid methyl ester) was selected as an organic surface-passivating material. MgO is a typical basic oxide which has high isoelectric point (~12.4), and, on the other hand, WO_3 has low isoelectric point (~0.5, typical acidic oxide) [20]. $PC_{61}BM$ is an n-type organic semiconductor which is widely used in P3HT/$PC_{61}BM$ bulk heterojunction photovoltaic devices [21,22]. $PC_{61}BM$ has a higher LUMO energy level (3.7 eV) compared to the position of TiO_2 conduction band (4.4 eV). It was expected that back transfer of injected electrons could be prohibited by $PC_{61}BM$ interlayer. The effect of these surface-passivating materials was evaluated in TiO_2-nanotube-based DSCs.

2. Experimental

TiO_2 nanotube arrays were fabricated by anodic oxidation of 0.5 mm thick Ti foil (99%, Alfar Aesar) in ethylene glycol solution containing 0.3 wt% NH_4F and 2 vol% H_2O. A constant potential 60 V with a ramping speed of 1 V s^{-1} was applied between an anode and a cathode. Pt metal was used as a counter electrode. Before anodization process, Ti foils were successively sonicated with acetone, ethanol, and DI water to remove the residue on the surface of Ti foils. As-anodized TiO_2 nanotube arrays were rinsed with DI water and annealed at 500 °C for 1 h. The pore size, wall thickness, and length of TiO_2 nanotube arrays were determined by field emission scanning electron microscopy (FESEM, Philips XL 30SFEG). Annealed TiO_2 nanotube arrays were analyzed by XRD (X-Ray Diffractometry, Rigaku D/MAX-RC, Cu Kα radiation) to confirm the crystallization of them.

Surface passivation of annealed TiO_2 nanotube arrays with MgO, WO_3, and $PC_{61}BM$ was done by using $Mg(CH_3COO)_2{\cdot}4H_2O$ (magnesium acetate pentahydrate, 99%, Junsei Chemical Co., Ltd.), $(NH_4)_{10}W_{12}O_{41}{\cdot}5H_2O$ (ammonium tungstate para pentahydrate, GR, Wako Pure Chemical Industries, Ltd.), and $PC_{61}BM$ powders (99.5%, Nano-C, Inc.) as precursors, respectively. Samples for MgO and WO_3 coating were immersed in aqueous solution by controlling the concentration of each precursor at 65 °C for 30 min. These samples were rinsed with DI water and annealed at 500 °C for 30 min to crystallize hydrous MgO and WO_3. Samples for $PC_{61}BM$ coating were immersed in $PC_{61}BM$-dissolved dichloromethane solution at room temperature. These samples were rinsed with dichloromethane after immersion process.

TiO_2-nanotube-photoelectrodes with and without surface-passivating layers were immersed at room temperature for ~1 d in an ethanol solution containing 3×10^{-4} M cis-bis(isothiocyanato)bis(2, 2′bipyridyl-4,4′dicarboxylato) ruthenium (II) bis-tetrabutylammonium (N719) dye. The dye-adsorbed photoelectrodes were rinsed with ethanol solution and were dried at room temperature. Pt coated FTO glasses as counter electrodes were prepared by spin coating 0.7 mM H_2PtCl_6 solution in 2-propanol at 500 rpm for 10 s and subsequently annealing at 380 °C for 30 min. Dye-adsorbed photoelectrodes and Pt coated FTO glasses were spaced by using 60 μm surlyn film purchased from DuPont Co., Ltd. The liquid electrolyte was prepared by dissolving 0.6 M 1-hexyl-2, 3-dimethylimidazolium iodide (C6DMIm), 0.05 M iodine, 0.1 M lithium iodide and 0.5 M 4-*tert*-butylpyridine in 3-methoxyacetonitrile. The *J–V* characteristics were measured under AM 1.5 G illumination (Keithley Model 2400 source measure unit). A 1000 W Xenon lamp (Oriel, 91193) was used as a light source. Electrochemical impedance spectroscopy (EIS) and V_{oc} decay behavior were measured by using VMP3 (Bio-Logic SAS). EIS measurement, in the frequency range swept from 100 kHz to 100 mHz, was conducted at V_{oc} condition under illumination.

3. Results and discussion

3.1. TiO_2 nanotube arrays fabricated by anodic oxidation

Highly ordered and robust TiO_2 nanotube arrays from Ti foil were obtained by anodic oxidation of Ti foil. Fig. 1 shows FESEM images of TiO_2 nanotube arrays fabricated by anodic oxidation in ethylene glycol solution containing 0.3 wt% NH_4F and 2 vol% H_2O. Fig. 1a shows ~15 μm-thick TiO_2 nanotube arrays. Fig. 1b shows the bottom image of TiO_2 nanotube arrays and TiO_2 nanotubes are hexagonally close-packed together. Their pore size, tube diameter, and wall thickness were ~60 nm, ~120 nm, and ~30 nm, respectively.

TiO_2 typically has various phases with fabrication methods. Anatase has been reported as the best phase for photoelectrodes of DSCs. To obtain the anatase TiO_2 nanotube arrays, as-anodized TiO_2 nanotube arrays were annealed. Fig. 2 shows X-ray diffraction (XRD) spectrum and FETEM image of TiO_2 nanotube arrays on Ti foil annealed at 500 °C for 1 h. Anatase peaks were shown together with Ti peaks in Fig. 2a. Lattice parameters measured by FETEM spots of Fig. 2b were well matched with anatase structure. These results revealed that amorphous as-anodized TiO_2 nanotube arrays were successfully crystallized into the anatase phase by annealing at 500 °C.

3.2. Inorganic surface passivation of TiO_2 nanotube arrays for DSCs

Fig. 3 shows *J–V* characteristic curves of DSCs which used surface-passivated TiO_2 nanotube arrays with inorganic materials (0.02 M MgO, 0.00001 M WO_3) as photoelectrodes. At each film thickness, the data showed similar behaviors. Photocurrents were scarcely changed by surface passivation. However, open circuit voltages (V_{oc}) were shifted positively or negatively by surface-passivating materials. MgO-coated solar cell shifted open circuit voltage to positive potential. On the other hand, WO_3-coated one shifted to negative potential.

These results are closely related to the shift of TiO_2 conduction band by surface passivation. It is well known that, in DSCs, the open circuit voltage is a difference of energy level between TiO_2 conduction band and liquid electrolyte. Surface passivation of TiO_2 nanotube arrays with a basic material such as MgO shifts TiO_2

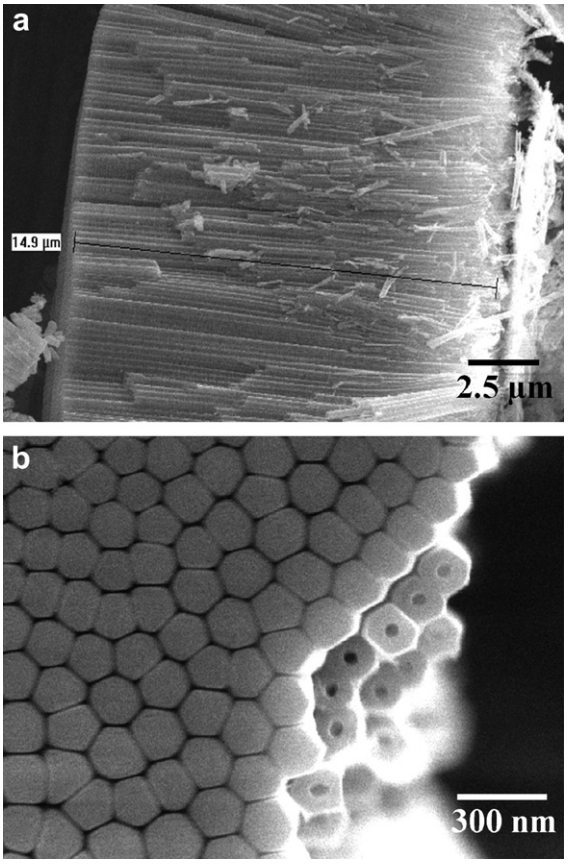

Fig. 1. FESEM images of TiO_2 nanotube arrays obtained by anodic oxidation of Ti foil at a constant potential 60 V in ethylene glycol solution containing 0.3 wt% NH_4F and 2 vol % H_2O at 30 °C for 1 h: (a) cross-sectional image of TiO_2 nanotube arrays; (b) bottom-image of TiO_2 nanotube arrays.

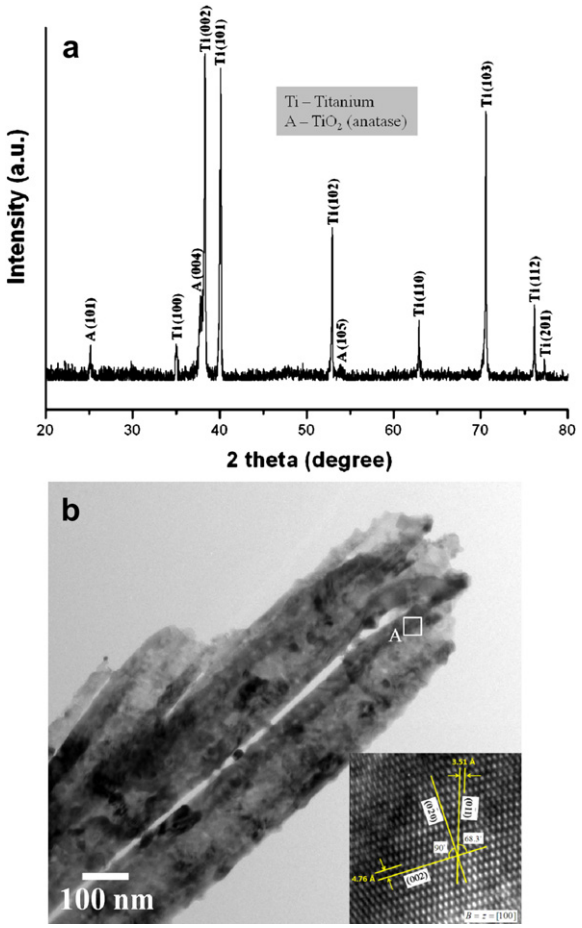

Fig. 2. X-ray diffraction pattern and FETEM images of annealed TiO_2 nanotube arrays at 500 °C for 1 h: (a) XRD pattern; (b) FETEM images (inset: a magnified image of part A).

conduction band to negative direction in DSCs. The difference of isoelectric point of TiO_2 and MgO leads to the difference of surface charge resulting in the formation of a dipole layer on the surface of photoelectrodes. The formation of a dipole layer shrinks the Fermi level to the positive direction due to the positive charge of MgO coating layer. At equilibrium, TiO_2 conduction band is shifted to negative direction by MgO coating layer. Shift of TiO_2 conduction band to negative direction increases the difference of energy level between TiO_2 conduction band and liquid electrolyte resulting in higher open circuit voltage. However, compared to the MgO coating, WO_3 coating has an opposite effect on the shift of TiO_2 conduction band. TiO_2 conduction band is positively shifted by WO_3 coating in DSCs. Therefore, the open circuit voltages of WO_3-coated samples were shifted to negative potential.

When the thickness of TiO_2 nanotube arrays was changed from 15 μm to 20 μm, photocurrents were increased and open circuit voltages were decreased. Photocurrents were increased due to the improvement of dye-adsorption in longer TiO_2 nanotube arrays. However, the decreased open circuit voltages were due to more chances of charge recombination. In the earlier report [9], the surface passivation of photoelectrode in DSCs with 5 μm-thick TiO_2 nanotube arrays was studied and dye-adsorption was greatly affected by surface-passivating materials. Basic materials such as MgO and ZnO enhanced dye-adsorption and its photocurrent is higher than an acidic material such as WO_3. These higher photocurrent and open circuit voltage by basic material coating improved the power conversion efficiency of DSCs. However, when the length of TiO_2 nanotube arrays was increased over 15 μm, the effect of surface passivation on photocurrent was attenuated and the thickness of TiO_2 nanotube arrays mainly affected the photocurrent. The power conversion efficiency is dependent on photocurrent and open circuit voltage. The photocurrent and open circuit voltage with thickness of TiO_2 nanotube arrays were increased and decreased, respectively. These two factors competitively act on the power conversion efficiency. As shown in Table 1, higher power

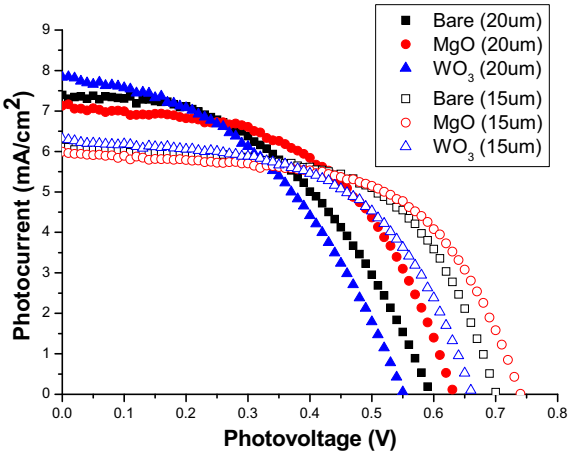

Fig. 3. *J–V* characteristic curves of DSCs based on bare, 0.02 M MgO-coated, and 0.00001 M WO_3-coated TiO_2 nanotube arrays.

Table 1
J–V characteristic values of DSCs based on bare, MgO-coated, and WO_3-coated TiO_2 nanotube arrays.

	Film thickness	J_{sc} (mA/cm^2)	V_{oc} (V)	Fill factor	Efficiency (%)
Bare	15 μm	6.11	0.70	0.60	2.55
MgO	15 μm	5.99	0.74	0.59	2.63
WO_3	15 μm	6.31	0.66	0.55	2.31
Bare	20 μm	7.40	0.59	0.47	2.05
MgO	20 μm	7.13	0.63	0.53	2.38
WO_3	20 μm	7.84	0.55	0.44	1.89

conversion efficiency of 2.63% in 15 μm-thick TiO_2 nanotube arrays was observed than 2.38% in 20 μm-thick TiO_2 nanotube arrays. In case of 15 μm-thick TiO_2 nanotube arrays, increasing of open circuit voltage is more effective on the power conversion efficiency of DSCs than decreasing of photocurrent by dye-adsorption.

V_{oc} decay measurements [3,23,24] of DSCs based on bare, MgO-coated and WO_3-coated nanotube arrays can be shown in Fig. 4. Fig. 4a shows raw data of V_{oc} decay measurements and Fig. 4b gives normalized V_{oc} decay measurements. In Fig. 4b, open circuit voltages of MgO-coated and WO_3-coated samples decayed more slowly than bare samples. From this result, it is considered that MgO and WO_3 layer have a blocking effect for charge recombination. However, in this study, the blocking effect of MgO and WO_3 layer had little influence on the improvement of DSCs.

Stability tests of MgO-coated and WO_3-coated samples need to be checked because coating layers can be etched by N719 dye molecules. It was reported that ZnO is etched by N719 dye molecules resulting in deterioration of DSCs [25]. Although Diamant et al. said that basic coating layers shift conduction band in negative direction [26], a direct proof that present conduction band shift by coating layers was not shown in this study. Stability tests of DSCs and extensive studies on band shift by coating layers are planned as future works.

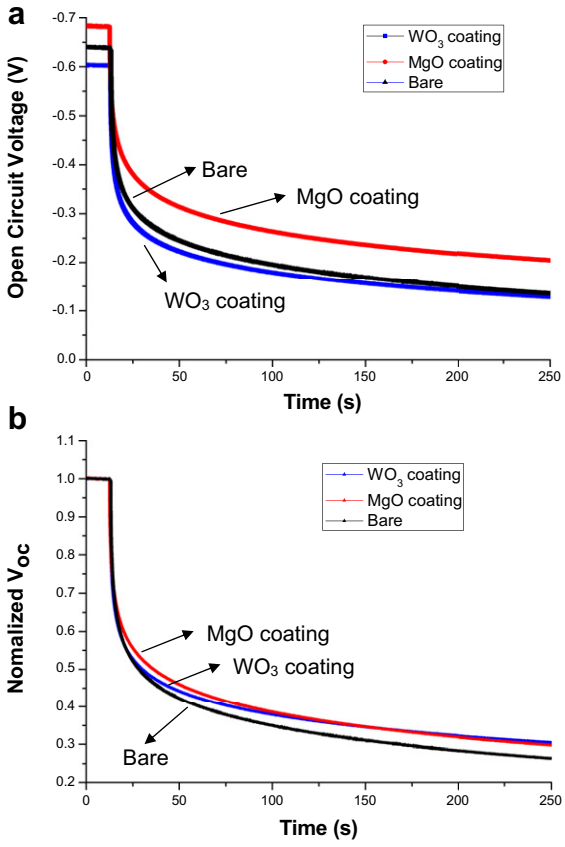

Fig. 4. V_{oc} decay measurements of DSCs based on bare, MgO-coated, WO_3-coated TiO_2 nanotube arrays: (a) raw data of V_{oc} decay measurements; (b) normalized V_{oc} decay measurements.

3.3. Surface passivation of TiO_2 nanotube arrays with an organic material ($PC_{61}BM$) and application to DSCs

Fig. 5 shows FETEM image of $PC_{61}BM$-coated TiO_2 nanotube arrays with an inset image of low magnification. Organic interlayer of $PC_{61}BM$ was conformally coated over steep topography of TiO_2 nanotube having 3D geometries and high-aspect ratio (HAR) and 3 nm-thick $PC_{61}BM$ interlayer was found on inner wall and outer wall of TiO_2 nanotubes.

Fig. 6 shows *J–V* characteristic curves of DSCs based on bare and $PC_{61}BM$-coated TiO_2 nanotube arrays. Photocurrents of $PC_{61}BM$-coated samples were enhanced. On the other hand, open circuit voltages were decreased by $PC_{61}BM$ coating. When the $PC_{61}BM$ concentration was increased up to 2 mg ml^{-1}, the effect of efficiency improvement was very weak. As shown in Table 2, when the $PC_{61}BM$ concentration was 3 mg ml^{-1}, optimum efficiency of 2.27% could be obtained by overcoming V_{oc} offset to negative potential.

It is considered that photocurrents of $PC_{61}BM$-coated samples were increased due to the double excitation of photoelectrons from both dye-molecules and $PC_{61}BM$ interlayer [27]. Band gap of $PC_{61}BM$ is ~2.4 eV and energy band of TiO_2 nanotube/$PC_{61}BM$ interlayer/dye has a step-like structure. Therefore, while most photoelectrons are being generated from dye-molecules, $PC_{61}BM$ interlayer can help charge generation mainly in the regime of short wavelength. It seems that low V_{oc} values of $PC_{61}BM$-coated samples are due to the strong acidity of $PC_{61}BM$. It was reported that a fullerene derivative called $PC_{61}BM$ has a low isoelectric point below 1 [28,29]. As mentioned before, V_{oc} can be shifted positively or negatively according to the isoelectric point of surface-passivating materials in DSCs. Low isoelectric point of $PC_{61}BM$ shifts TiO_2 conduction band to positive direction and gives lower V_{oc} value compared to bare samples. This result exactly coincides with the former case of WO_3 coating.

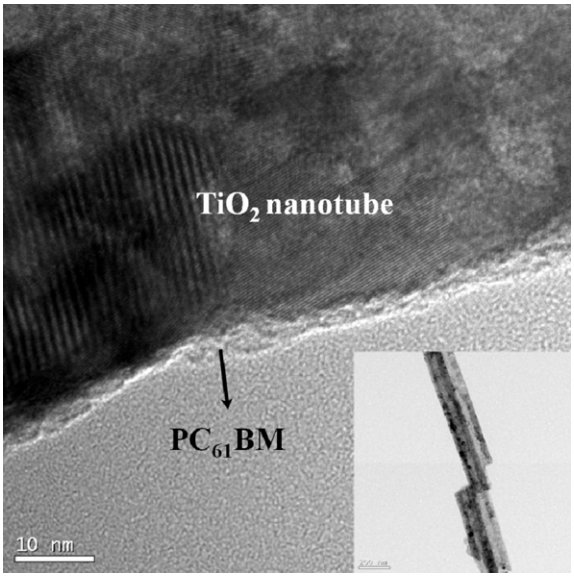

Fig. 5. FETEM image of $PC_{61}BM$-coated TiO_2 nanotube arrays (inset: a low magnified image).

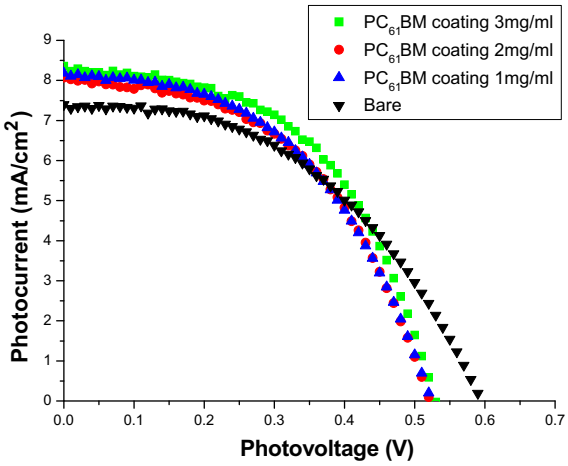

Fig. 6. *J–V* characteristic curves of DSCs based on bare and $PC_{61}BM$-coated TiO_2 nanotube arrays.

Fig. 7 gives V_{oc} decay results of DSCs based on bare and $PC_{61}BM$-coated TiO_2 nanotube arrays. Fig. 7a is raw data of V_{oc} decay measurements and Fig. 7b is normalized V_{oc} decay measurements. It could be found that these results were very similar to the behavior of Fig. 4. V_{oc} decay of $PC_{61}BM$-coated samples was slower than bare samples. This means that an electron lifetime in $PC_{61}BM$-coated samples is longer than that in bare samples. From V_{oc} decay results, we could conclude that $PC_{61}BM$ interlayer also had a blocking effect which retards back-transfer of injected photoelectrons.

$PC_{61}BM$ interlayer enhanced charge injection into TiO_2 films and had a blocking effect for charge recombination although V_{oc} values were slightly decreased. Increased photocurrents by $PC_{61}BM$ interlayer overcame V_{oc} offset to negative potential and improved the power conversion efficiency of DSCs. It has been reported that blocking back-transfer of photoelectrons not only reduces charge recombination between TiO_2 films and liquid electrolyte but also improves V_{oc} [8,19]. However, V_{oc} was decreased by $PC_{61}BM$ interlayer despite of its blocking effect. In case of $PC_{61}BM$ coating, the effect of isoelectric point was more dominant than that of blocking effect.

3.4. Effects of surface passivation of photoelectrodes in DSCs

There are several roles of surface-passivating layer in DSCs. Firstly, surface-passivating layer reduces charge recombination between TiO_2 films and liquid electrolyte [5,8,15,19]. Electrons in TiO_2 films usually resides at surface trap states [30]. Charge recombination mainly occurs at the surface trap states by reacting with I_3^- in liquid electrolyte. Surface-passivating layer, which has higher energy level of conduction band or LUMO than that of TiO_2 conduction band, blocks the path for charge recombination. It was

Table 2
J–V characteristic values of DSCs based on bare and $PC_{61}BM$-coated TiO_2 nanotube arrays.

	Film thickness	J_{sc} (mA/cm^2)	V_{oc} (V)	Fill factor	Efficiency (%)
Bare	20 μm	7.40	0.59	0.47	2.05
$PC_{61}BM$ coating (1 mg ml^{-1})	20 μm	8.18	0.52	0.48	2.07
$PC_{61}BM$ coating (2 mg ml^{-1})	20 μm	8.07	0.52	0.49	2.08
$PC_{61}BM$ coating (3 mg ml^{-1})	20 μm	8.36	0.53	0.51	2.27

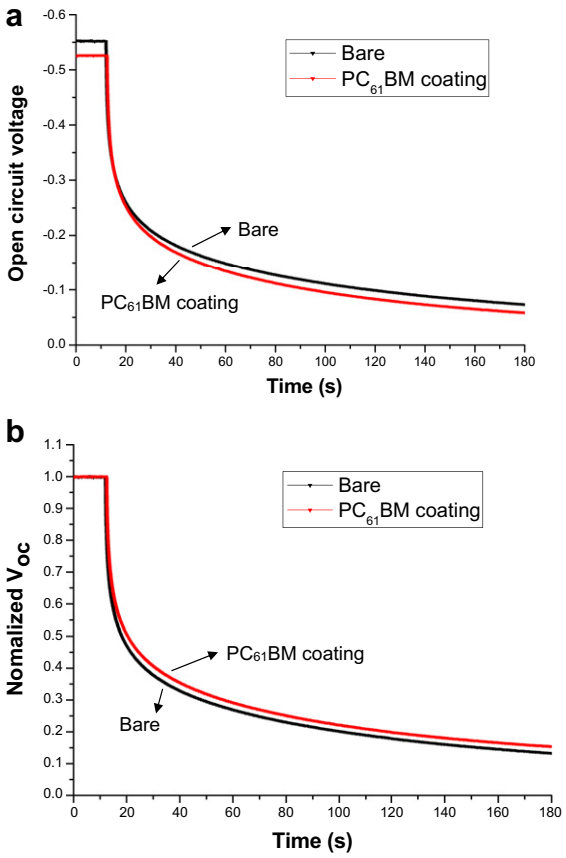

Fig. 7. V_{oc} decay measurements of DSCs based on bare and $PC_{61}BM$-coated TiO_2 nanotube arrays: (a) raw data of V_{oc} decay measurements; (b) normalized V_{oc} decay measurements.

also reported that surface trap sites in TiO_2 films were decreased by surface-passivating layer [15]. Secondly, surface passivation of photoelectrodes is closely related to dye adsorption by introducing the concept of isoelectric point [8,9,16,18,19]. If surface-passivating materials have a higher isoelectric point (pI >7) than TiO_2, the surface of photoelectrodes is positively charged during immersion process in N719 ethanol solution. Positively charged surface enhances dye-adsorption due to the attraction between negatively charged dye molecules and the surface of TiO_2 nanotube photoelectrodes. However, surface passivation of photoelectrodes with acidic materials (pI <7) can give a deteriorated effect on the dye adsorption. Dye adsorption can also be improved due to the increase of surface area of photoelectrodes by surface-passivating layer. Thirdly, TiO_2 conduction band, as shown in Fig. 8, can be shifted to positive or negative direction by surface-passivating layer [16,26]. The band shift of photoelectrodes is due to the formation of surface dipole layer at the interface resulting from differences between TiO_2 and surface-passivating materials with respect to their acidity or electron affinity [26]. Surface passivation with basic materials shifts TiO_2 conduction band to negative direction. On the other hand, acidic materials shifts TiO_2 conduction band to positive direction. Therefore, it is expected that higher V_{oc} can be obtained by surface passivation of photoelectrodes with basic materials. Finally, if surface-passivating materials have a low band gap similar to dye-molecules and energy band of TiO_2/surface-passivating layer/dye has a step-like structure, surface-passivating interlayer can help charge generation enhancing photocurrents of DSCs. All these effects cannot be obtained all the time. The power conversion efficiency depends on which effects are dominant.

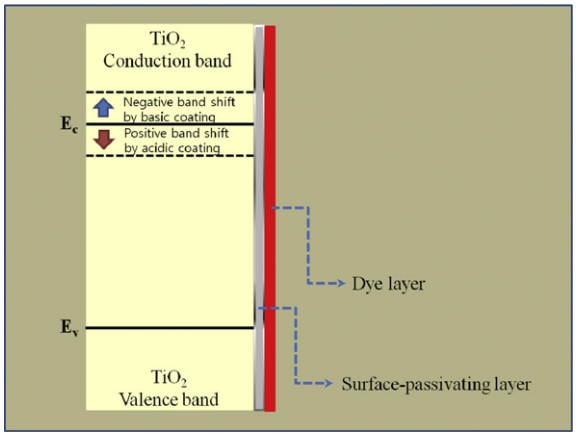

Fig. 8. Schematic diagram of TiO_2 conduction band shift with surface-passivating layers.

4. Conclusion

Surface passivation of TiO_2 nanotube arrays with organic and inorganic materials was introduced to improve the power conversion efficiency of DSCs. Open circuit voltage was affected by acidity of surface-passivating materials. When the isoelectric point of surface-passivating materials was higher than 7, TiO_2 conduction band was shifted to negative direction resulting in increased V_{oc}. On the other hand, when the photoelectrodes were coated by acidic materials, open circuit voltages were decreased. In case of inorganic coating such as MgO and WO_3, V_{oc} shift by surface-passivating materials gave a direct influence on the performance of DSCs. Photocurrents were scarcely changed by surface passivation of inorganic materials. However, when photoelectrodes were coated with a fullerene derivative called $PC_{61}BM$, photocurrents were enhanced although V_{oc} was slightly decreased. It was concluded that increased photocurrents by $PC_{61}BM$ coating was due to the double excitation of photoelectrons from both dye molecules and $PC_{61}BM$ interlayer, and V_{oc} shift by $PC_{61}BM$ coating to negative potential was due to the low isoelectric point (pI <1) of $PC_{61}BM$. It is expected that further improvement would be fulfilled by finding surface-passivating materials which have a similar position of energy band with $PC_{61}BM$ and also have a high isoelectric point (pI >7). Stability tests of surface-passivated samples and extensive studies on band shift by coating layers are planned as future works.

Acknowledgments

This research was financially supported by the Ministry of Education, Science Technology (MEST) and National Research Foundation of Korea (NRF) through the Human Resource Training Project for Regional Innovation and the National Research Foundation of Korea (NRF) grant funded by the Korea government (MEST) (No. 2010-0026916).

References

[1] B. O'regan, M. Gratzel, Nature 353 (1991) 737–740.
[2] M.A. Green, K. Emery, Y. Hishikawa, W. Warta, Prog. Photovolt.: Res. Appl. 19 (2011) 84–92.
[3] G.K. Mor, K. Shankar, M. Paulose, O.K. Varghese, C.A. Grimes, Nano Lett. 6 (2006) 215–218.
[4] K. Zhu, N. Neale, A. Miedaner, A. Frank, Nano Lett. 7 (2007) 69–74.
[5] S.H. Kang, J.Y. Kim, Y. Kim, H.S. Kim, Y.E. Sung, J. Phys. Chem. C 111 (2007) 9614–9623.
[6] B. Lei, J. Liao, R. Zhang, J. Wang, C. Su, D. Kuang, J. Phys. Chem. C 114 (2010) 15228–15234.
[7] H. Park, W. Kim, H. Jeong, J. Lee, H. Kim, W. Choi, Sol. Energy Mater. Sol. Cells 95 (2011) 184–189.
[8] H. Park, D.J. Yang, H.G. Kim, S.J. Cho, S.C. Yang, H. Lee, W.Y. Choi, J. Electroceram. 23 (2009) 146–149.
[9] H. Park, D.J. Yang, J.S. Yoo, K.S. Mun, W.R. Kim, H.G. Kim, W.Y. Choi, J. Ceram. Soc. Jpn. 117 (2009) 596–599.
[10] D.J. Yang, H. Park, S.J. Cho, H.G. Kim, W.Y. Choi, J. Phys. Chem. Solids 69 (2008) 1272–1275.
[11] S. Kang, S. Choi, M. Kang, J. Kim, H. Kim, T. Hyeon, Y. Sung, Adv. Mater. 20 (2008) 54–58.
[12] M. Adachi, Y. Murata, J. Takao, J. Jiu, M. Sakamoto, F. Wang, J. Am. Chem. Soc. 126 (2004) 14943–14949.
[13] S. Yang, D. Yang, J. Kim, J. Hong, H. Kim, I. Kim, H. Lee, Adv. Mater. 20 (2008) 1059–1064.
[14] G. Mor, O. Varghese, M. Paulose, K. Shankar, C. Grimes, Sol. Energy Mater. Sol. Cells 90 (2006) 2011–2075.
[15] P. Cheng, C. Deng, X. Dai, B. Li, D. Liu, J. Xu, J. Photochem. Photobiol. A: Chem. 195 (2008) 144–150.
[16] Y. Diamant, S.G. Chen, O. Melamed, A. Zaban, J. Phys. Chem. B 107 (2003) 1977–1981.
[17] B. Gregg, F. Pichot, S. Ferrere, C. Fields, J. Phys. Chem. B 105 (2001) 1422–1429.
[18] I. Hod, M. Shalom, Z. Tachan, S. Ruhle, A. Zaban, J. Phys. Chem. C 114 (2010) 10015–10018.
[19] H. Jung, J. Lee, M. Nastasi, S. Lee, J. Kim, J. Park, K. Hong, H. Shin, Langmuir 21 (2005) 10332–10335.
[20] G.A. Parks, Chem. Rev. 65 (1965) 177–198.
[21] J. Kim, K. Lee, N. Coates, D. Moses, T. Nguyen, M. Dante, A. Heeger, Science 317 (2007) 222–225.
[22] G. Yu, J. Gao, J.C. Hummelen, F. Wudl, A.J. Heeger, Science 270 (1995) 1789–1791.
[23] F. Fabregat-Santiago, J. García-Cañadas, E. Palomares, J.N. Clifford, S.A. Haque, J.R. Durrant, G. Garcia-Belmonte, J. Bisquert, J. Appl. Phys. 96 (2004) 6903–6907.
[24] A. Zaban, M. Greenshtein, J. Bisquert, ChemPhysChem 4 (2003) 859–864.
[25] F. Yan, L. Huang, J. Zheng, J. Huang, Z. Lin, F. Huang, M. Wei, Langmuir 26 (2010) 7153–7156.
[26] Y. Diamant, S. Chappel, S. Chen, O. Melamed, A. Zaban, Coord. Chem. Rev. 248 (2004) 1271–1276.
[27] S. Cook, R. Katoh, A. Furube, J. Phys. Chem. C 113 (2009) 2547–2552.
[28] D. Bouchard, X. Ma, C. Isaacson, Environ. Sci. Technol. 43 (2009) 6597–6603.
[29] X. Ma, D. Bouchard, Environ. Sci. Technol. 43 (2009) 330–336.
[30] J. van de Lagemaat, N.G. Park, A.J. Frank, J. Phys. Chem. B 104 (2000) 2044–2052.